

Efficient UV-Blue Photoluminescing Thiol-Stabilized Water-Soluble Alloyed ZnSe(S) Nanocrystals

Alexey Shavel, Nikolai Gaponik,[†] and Alexander Eychmüller*

Institute of Physical Chemistry, University of Hamburg, Grindelallee 117, 20146 Hamburg, Germany

Received: December 19, 2003; In Final Form: March 5, 2004

The aqueous synthesis and post-preparative treatment of thiol-stabilized ZnSe colloidal nanocrystals (2–3 nm in size) have been studied. The post-preparative irradiation of the nanoparticles improves their luminescence properties leading to strong (up to 25–30% photoluminescence quantum yield) band gap UV-blue emission. The irradiation results in an incorporation of sulfur into the particles and in the formation of ZnSe(S) alloyed nanocrystals. The ZnSe(S) nanocrystals obtained were used for the fabrication of UV-blue-emitting layer-by-layer assembled films with a PL maximum at ca. 390 nm.

Introduction

Chemically synthesized semiconductor nanocrystals (or colloidal quantum dots (QDs)) have attracted considerable interest during the past decade. Narrow and intensive emission spectra, continuous absorption bands, high chemical and photobleaching stability, processability, and surface functionality are among the most attractive properties of these materials. The properties of the QDs depend strongly on the type of the nanocrystals, the size (quantum-confinement), and the capping agent, thus they can be tuned by a proper choice of the synthetic conditions. There is a wide range of very efficiently light-emitting QDs which can be synthesized both in organic media or as aqueous solutions. Worth mentioning are CdSe,^{1,2} InP,³ CdTe⁴ (visible light region), PbSe,^{5,6} HgTe,⁷ and InAs⁸ (near-infrared and infrared region). At the same time, reports on QDs efficiently emitting in the UV-blue spectral region (below 500 nm) are less common. Among them, mainly CdS,⁹ CdSe,¹⁰ and ZnSe^{11,12,13} QDs have to be mentioned. To the best of our knowledge, the only successful synthesis of strongly UV-blue-emitting ZnSe was done by an organometallic approach in a TOP–HDA mixture.¹³ At the same time, the photoluminescence (PL) quantum efficiencies (QE) achieved for ZnSe particles' aqueous syntheses^{11,12} were reported to be less than 1%.

It is well-known that the optical properties and, in particular, the PL QE of as-prepared colloidal QDs can be improved post-preparatively. The creation of inorganic shells,^{14,15} size-selective precipitation,^{4,16} and the change of solution properties (e.g., pH)^{4,17} are methods for obtaining strong-luminescing nanocrystals. Recently, photoassisted methods of post-preparative QDs' treatment were shown to be powerful to improve the PL QE. Worth mentioning are the photoetching of thiol-capped CdTe,⁴ TOPO-capped CdSe/CdS/ZnS nanorods,¹⁸ citric acid-capped CdSe,¹⁹ or the photochemical etching in the presence of HF of TOPO-capped InP.²⁰ A moderate (3–10 times) improvement of the PL QE for the CdTe QDs and the nanorods as well as a drastic improvement in the cases of CdSe and InP (hundreds of times) were shown to be possible.

Here we report on the optimization of the synthesis of thiol-stabilized ZnSe nanocrystals and their post-preparative photochemical treatment leading to strong UV-emission.

Experimental Section

All chemicals used were of analytical grade or of the highest purity available. All solutions were prepared using Milli-Q water (Millipore) as the solvent. Al₂Se₃ lumps (Alfa Aesar) were used as the source of H₂Se. Thioglycerol (TG), thioglycolic acid (TGA), and 3-mercaptopropionic acid (MPA) were purchased from Sigma-Aldrich and were used as capping agents without additional purification.

In a typical synthesis, 0.875 g (2.35 mmol) of Zn(ClO₄)₂·6H₂O was dissolved in 125 mL of water, and 5.7 mmol of the thiol stabilizer (thioglycerol, thioglycolic acid, or 3-mercaptopropionic acid) were added under stirring, followed by adjusting the pH by dropwise addition of 1 M solution of NaOH to 6.5 in the case of TGA or MPA capping, or to 11.2–11.8 in the case of TG. The mentioned pH values were experimentally found to be optimal for the synthesis of stable colloids. The solution was placed in a three-necked flask fitted with a septum and valves, and it was deaerated by N₂ bubbling for 1 h. Under stirring, H₂Se gas (generated by the reaction of 0.134 g (0.46 mmol) of Al₂Se₃ lumps with an excess amount of 1 N H₂SO₄ under N₂ atmosphere) was passed through the solution together with a slow nitrogen flow for nearly 20 min. ZnSe precursors were formed at this stage. The further nucleation and growth of the nanocrystals proceeded on refluxing at 100 °C under open-air conditions with a condenser attached.

The photochemical treatment of the samples was done with a 100 W xenon lamp with a water filter to cut off the NIR part of the spectrum. The intensity of the light was approximately 200 mW/cm² (measured by a Powerlitemeter C5100 (Continuum) with a PowerMax PM30V2 detector). UV–vis absorption spectra were recorded with a Cary 50 spectrophotometer (Varian). PL measurements were performed at room temperature using a FluoroMax-2 spectrofluorimeter (Instruments SA). The room-temperature PL QE of the ZnSe nanocrystals was estimated following the procedure of ref 21 by comparison with quinine (Fluka) in 1 N H₂SO₄ solution assuming its PL QE to be 51%. High-resolution transmission electron microscopy (HRTEM) and energy-dispersive X-ray analysis (EDX) were

* Author to whom correspondence should be addressed. E-mail: eychmuel@chemie.uni-hamburg.de.

[†] On leave from Physico-Chemical Research Institute, Belarussian State University, 220050 Minsk, Belarus.

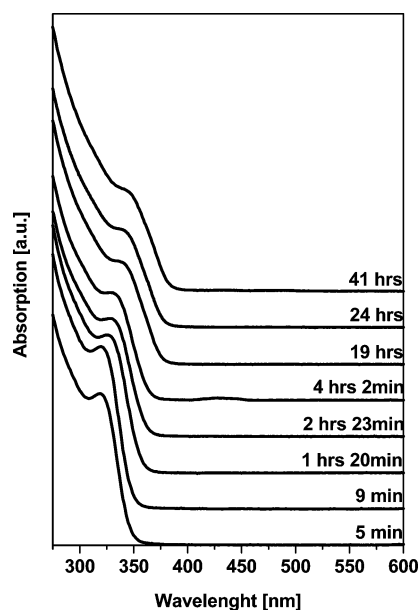


Figure 1. Evolution of the absorption spectra of a crude solution of ZnSe NCs during the synthesis.

performed on a Philips CM-300 microscope operating at 300 kV. TEM samples were prepared by dropping diluted solutions ($\text{H}_2\text{O}/\text{DMF} = 1:10$) of ZnSe nanocrystals onto 400-mesh carbon-coated copper grids with the excessive solvent immediately evaporated. A mixture with DMF was chosen to facilitate uniform drying of the drop on the hydrophobic grid surface. Powder X-ray diffraction (XRD) measurements were carried out with a Philips X'Pert diffractometer (Cu $K\alpha$ radiation, variable entrance slit, Bragg–Brentano geometry, secondary monochromator). Samples for this study were prepared by placing finely dispersed powders of ZnSe nanocrystals on standard Si supports. For preparation of the layer-by-layer (LbL) assembled films poly(diallyldimethylammonium chloride) (PDDA, Mw 100,000–200,000, Aldrich) and poly(ethylenimine) (PEI, Aldrich) were used.

Results and Discussion

A typical temporal evolution of the absorption of the ZnSe QDs is shown in Figure 1. A growth of the NCs during reflux is indicated by a low-energy shift of the absorption. The PL of these solutions is negligible and shows mainly a broad trap emission band (400–600 nm). An additional very weak band-edge emission appears only after long times of reflux. It is mentioned that among the capping agents used, a relatively stronger trap-emission is found to be characteristic for TG-capped ZnSe QDs. The synthesis and characterization of this type of whitish-blue-emitting QDs with PL QE being below 1% was reported recently.¹¹

To improve the PL properties of the ZnSe NCs (enhancement of the band-edge and suppression of the trap-emission), the colloidal solutions were irradiated with the “white light” of a 100 W xenon lamp. The photochemical treatment was performed as follows. The solutions were exposed to the light, and aliquots of them were taken for spectroscopic measurements after different periods of time. The dependence of the PL spectra on the duration of the irradiation is shown in Figure 2. After several hours under illumination, the PL QE increases from near-zero ($\leq 0.1\%$) being characteristic for the as-prepared solutions up to 10–30% depending on the conditions used. Being removed from the irradiation, the colloids showed a reasonable stability. Several months of storage in the dark under air resulted neither

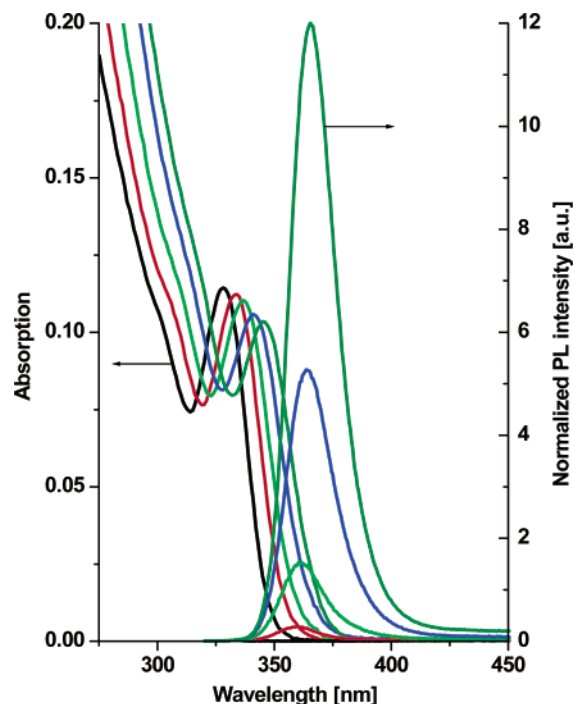


Figure 2. Changes in the absorption and PL properties during irradiation with white light (xenon lamp, 100 W with a water filter to cut off the NIR part of the spectrum). Total irradiation time: near 6 h.

in coagulation nor in recognizable changes in the optical properties. It should be mentioned that ZnSe QDs capped with TGA, MPA, or TG showed a similar increase in PL efficiency. However, for both MPA- and TG- capped QDs, a pronounced increase also of the trap-emission band under irradiation is observed. Therefore, only the TGA-capped QDs were chosen for more detailed studies.

To understand the nature of the photoinduced processes, the influence of the chemical composition of the solution on the resulting PL QE was studied. The ZnSe QDs were precipitated from the crude solution by addition of a nonsolvent (2-propanol) and subsequent centrifugation. The precipitate was separated from the supernatant and was redissolved in pure water, giving a stable colloidal solution with its optical properties being generally similar to the initial one. Purified by this way, the QDs were used for preparation of 3 different solutions (S1–S3, see Table 1). In addition, the crude solution of NCs was divided into fractions with narrower size distribution (by size-selective precipitation technique¹⁶), and one of the fractions was used for the preparation of solution S4. The experiments with these solutions as well as with the crude solution (S0) were done under the same conditions and were repeated 3 times to avoid possible mistakes and to confirm reproducibility.

As is seen from Table 1, the phototreatment of the ZnSe QDs proceeds efficiently only in the presence of an excess amount of both capping-agent and Zn^{2+} ions in solution. Note that free unreacted stabilizer molecules and Zn^{2+} ions are present also in the crude solution because they are used in excess over the Se source (see above the reaction recipe).

As is seen from Figure 2, the PL efficiency of the TGA-capped QDs increases solely due to the appearance of a pronounced narrow band gap emission band, while the trap-associated emission is negligible. The position of the PL maximum and the absorption edge shifted to the lower energy region, which is in contrast to the high-energy shift observed recently for the photoetching of thiol-stabilized CdTe nanocrystals.⁴ Since the QDs studied are in the regime of size-

TABLE 1: Chemical Composition of the QDs Solutions Used for Irradiation (pH 6.5 by adding NaOH)

sample number	ZnSe QDs, mmol/L (ref to Se)	TGA, mmol/L	Zn ²⁺ , mol/L (in form of Zn(ClO ₄) ₂)	result of phototreatment
S0 (crude)	10.2	not added	not added	stable; PL QE of up to 10%
S1	10.2			coagulation after 10 min; no improvement of PL QE
S2	10.2	42.2		stable; increase of PL QE is negligible
S3	10.2	42.2	17.4	stable; PL QE of up to 10%
S4 (selected fraction)	10.2 ^a	42.2	17.4	stable; PL QE of up to 25–30%

^a The absorption is equal to the crude solution in the region of the first excitonic maximum.

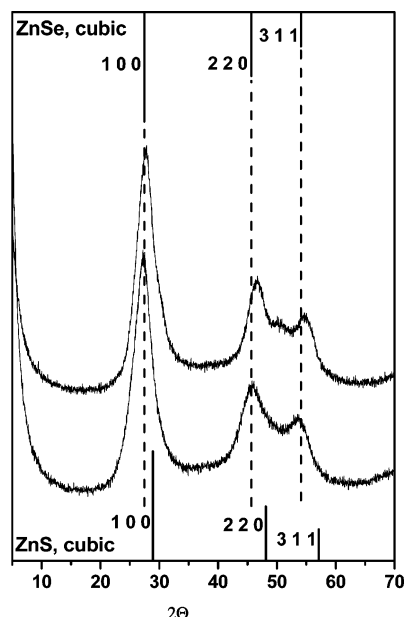


Figure 3. XRD patterns of ZnSe NCs before (down) and after (up) irradiation by white light. The line spectra show the cubic ZnSe and ZnS reflection with their relative intensities.

confinement, i.e., a low-energy band edge corresponds to larger particles, we can assume that the colloidal ZnSe particles grow under irradiation. These findings, together with the data of Table 1, allow us to consider that the growth proceeds not through the Ostwald ripening mechanism but instead consumes mainly Zn²⁺ ions and TGA from the solution. In the case of Ostwald ripening, the smaller particles in an ensemble dissolve giving the “monomer” species for the growth of the larger ones. It is noted that the observed evolution of the PL properties of the ZnSe(S) NCs is generally followed by a decrease of the Stokes shift.

The appearance of the strong band-gap emission and the small level of the trap-associated one allow us to suggest that such a photoinduced growth is accompanied with a transition of the nanoparticles in the direction of sulfur-enriched alloyed particles. Moreover, the small level of surface trap emission can be a result of the formation of an efficient passivating shell. More detailed information can be obtained from the XRD and TEM data (Figures 3 and 4). The positions of the XRD peaks exhibit a small shift from their normal position for the ZnSe structure. EDX data show that the content of sulfur continually rises during the irradiation from 19 at. % before to 29 at. % after the process (the sulfur in the EDX data of the initial samples appears mainly due to the stabilizer (TGA)). Indeed, the particles' growth under these conditions can proceed only by involving the sulfur as a chalcogenide source, which appears as a product of the photodecomposition or hydrolysis of the thioglycolic acid in solution. As a result, the XRD lines shift to values which are characteristic for ZnSe–ZnS alloys, i.e., located between the positions of the corresponding lines for pure ZnSe and ZnS

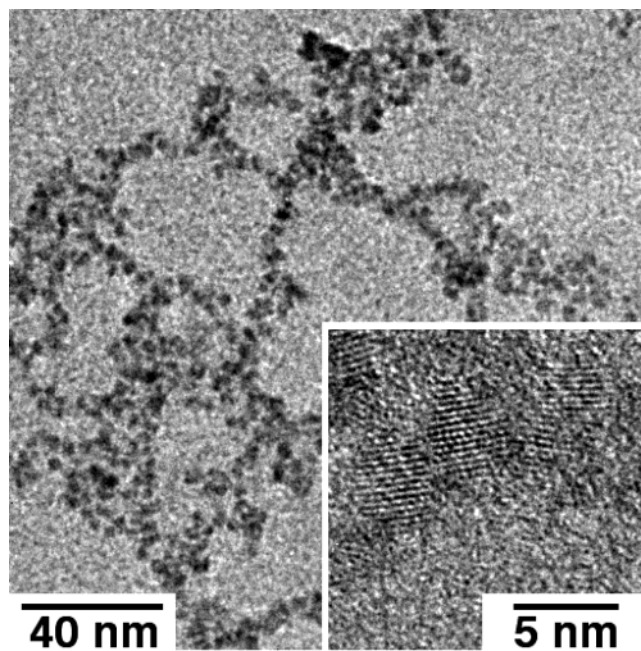


Figure 4. High-resolution transmission electron microscopy (HRTEM) image of luminescent ZnSe(S) NCs.

(Figure 3). Such a kind of XRD-spectrum evolution accompanied also the growth of thiol-stabilized CdTe(S) QDs as reported in detail recently.^{4,22} The sulfur-enriched phase forms during the phototreatment as a kind of alloyed shell on the surface of the preformed ZnSe particles cores, followed by a reorganization of the particles structure and in this way the content of sulfur increases toward the surface of the nanoparticles. The formation of such an alloyed shell constructed from larger band gap material can explain the improvement of the optical properties (higher PL QE and stability).^{4,22}

It has to be emphasized that distinctions between true core–shell and the above-mentioned alloyed crystals with a gradient of the sulfur content are probably not possible from the point of view of their physical properties. In fact, such small crystals (2–3 nm in size) have only a few lattice planes per crystal (the lattice constant *a* is near 0.56 nm for the ZnSe cubic structure, see also Figure 4). From this, a removal and/or intermixing of a second chalcogenide into the surface layer (S) leads almost automatically to an alloyed crystal structure.

To demonstrate the processability of the ZnSe(S) NCs their assembly into layer-by-layer (LbL) thin films has been performed. Poly(diallyldimethylammonium chloride) and poly(ethylenimine) were used as oppositely charged polyelectrolytes for the LbL film formation. LbL films on planar surfaces have been prepared using carefully cleaned quartz slides as substrates. The following standard cyclic procedure was employed, (i) dipping of the substrate into a solution of polyelectrolyte (5 mg/mL in 0.5 M NaCl) for 10 min (PEI was used for the first layer and PDDA for the 2nd and further layers²³); (ii) rinsing with water for 1 min; (iii) dipping into aqueous dispersions of

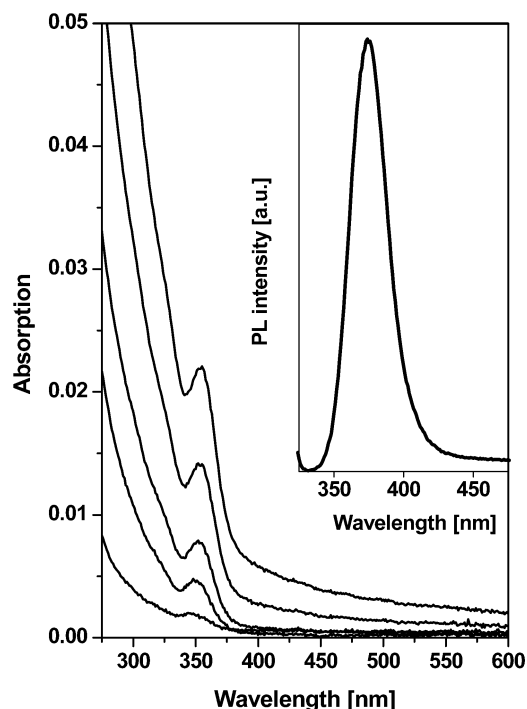


Figure 5. Evolution of the absorption spectra during the layer-by-layer (LbL) assembly of PDDA-ZnSe films. Inset: PL spectra of a 5 layer LbL film ($\lambda_{\text{ex}} = 300$ nm).

the nanocrystals for 20 min; (iv) rinsing with water again for 1 min. On each surface exposed, such a procedure resulted in a “bilayer” consisting of a polymer/NCs composite. The cycle can be repeated as many times as necessary to obtain a multilayer film of desirable thickness. The thickness of the LbL film strongly depends on the number of “bilayers”. Moreover, a linear dependence of the absorption in the region of the first absorption maximum on the number of bilayers (up to 7 bilayers) was observed. The absorption and PL properties of the LbL structures are shown in Figure 5.

Summary

An aqueous synthesis of thiol-stabilized ZnSe NCs has been investigated. A post-preparative photochemical treatment giving rise to strong (up to 25–30% PL QE) band gap luminescence has been developed. The changes in particle composition, size, and crystal structure accompanying the irradiation are discussed.

The ZnSe NCs obtained were used for the fabrication of efficiently UV-blue-emitting layer-by-layer assembled films with a PL maximum at ca. 390 nm.

Acknowledgment. We acknowledge Dmitri Talapin, Horst Weller, and Andreas Kornowski for useful discussions, and the latter also for taking the TEM images. This work was supported by the German Science Foundation (DFG SPP 1072) and the EU-project “Funlight”.

References and Notes

- (1) Alivisatos, A. P. *J. Phys. Chem.* **1996**, *100*, 13226.
- (2) Murray, C. B.; Norris, D. J.; Bawendi, M. G. *J. Am. Chem. Soc.* **1993**, *115*, 8706.
- (3) Mičić, O. I.; Sprague, J.; Lu, Z.; Nozik, A. J. *Appl. Phys. Lett.* **1996**, *68*, 3150.
- (4) Gaponik, N.; Talapin, D. V.; Rogach, A. L.; Hoppe, K.; Shevchenko, E. V.; Kornowski, A.; Eychmüller, A.; Weller, H. *J. Phys. Chem.* **2002**, *106*, 7177.
- (5) Wehrenberg, B. L.; Wang, C.; Guyot-Sionnest, P. *J. Phys. Chem. B* **2002**, *106*, 10634.
- (6) Du, H.; Chen, C.; Krishnan, R.; Krauss, T. D.; Harbold, J. M.; Wise, F. W.; Thomas, M. G.; Silcox, J. *Nano Lett.* **2002**, *2*, 1321.
- (7) Rogach, A.; Kershaw, S.; Burt, M.; Harrison, M.; Kornowski, A.; Eychmüller, A.; Weller, H. *Adv. Mater.* **1999**, *11*, 552.
- (8) Cao, Y.-W.; Banin, U. *J. Am. Chem. Soc.* **2000**, *122*, 9692.
- (9) Spanhel, L.; Haase, M.; Weller, H.; Henglein, A. *J. Am. Chem. Soc.* **1987**, *109*, 5649.
- (10) Talapin, D. V.; Rogach, A. L.; Mekis, I.; Haubold, S.; Kornowski, A.; Haase, M.; Weller, H. *Colloids Surf. A* **2002**, *202*, 145.
- (11) Murase, N.; Gao, M. Y.; Gaponik, N.; Yazawa, T.; Feldmann, J. *Int. J. Modern Phys. B* **2001**, *15*, 3881.
- (12) Nikesh, V. V.; Mahamuni, S. *Semicond. Sci. Technol.* **2001**, *16*, 687.
- (13) Hines, M. A.; Guyot-Sionnest, P. *J. Phys. Chem. B* **1998**, *102*, 3655.
- (14) Dabbousi, B. O.; Rodriguez-Viejo, J.; Mikulec, F. V.; Heine, J. R.; Mattoussi, H.; Ober, R.; Jensen, K. F.; Bawendi, M. G. *J. Phys. Chem. B* **1997**, *101*, 9463.
- (15) Peng, X.; Schlamp, M. C.; Kadavanich, A. V.; Alivisatos, A. P. *J. Am. Chem. Soc.* **1997**, *119*, 7019.
- (16) Talapin, D. V.; Rogach, A. L.; Shevchenko, E. V.; Kornowski, A.; Haase, M.; Weller, H. *J. Am. Chem. Soc.* **2002**, *124*, 5782.
- (17) Gao, M.; Kirstein, S.; Möhwald, H.; Rogach, A. L.; Kornowski, A.; Eychmüller, A.; Weller, H. *J. Phys. Chem. B* **1998**, *102*, 8360.
- (18) Manna, L.; Scher, E. C.; Li, L.-S.; Alivisatos, A. P. *J. Am. Chem. Soc.* **2002**, *124*, 7136.
- (19) Wang, Y.; Tang, Z.; Correa-Duarte, M. A.; Liz-Marzan, L. M.; Kotov, N. A. *J. Am. Chem. Soc.* **2003**, *125*, 2830.
- (20) Talapin, D. V.; Gaponik, N.; Borchert, H.; Rogach, A. L.; Haase, M.; Weller, H. *J. Phys. Chem. B* **2002**, *106*, 12659.
- (21) Demas, J. N.; Crosby, G. A. *J. Phys. Chem.* **1971**, *75*, 991.
- (22) Rogach, A. L. *Mater. Sci. Eng. B* **2000**, *69–70*, 435.
- (23) Gao, M.; Lesser, C.; Kirstein, S.; Möhwald, H.; Rogach, A. L.; Weller, H. *J. Appl. Phys.* **2000**, *87*, 2297.